The pyroxenes of the alkaline igneous complexes of eastern Uganda

By RUTH C. TYLER

62 Hallgarth St., Durham[1]

and B. C. KING

Bedford College, London N.W.1

[Read 3 June 1965]

Summary. Chemical analyses, some optical data, and specific gravities are given for 57 pyroxenes from the alkaline rocks of Uganda. They are members of the diopside–hedenbergite–acmite series, the more diopsidic varieties occurring in rocks of the ijolite series and the more acmitic in syenites and carbonatites. TiO_2 is highest in those pyroxenes from rocks that do not contain melanite. The refractive indices and specific gravities are controlled by the Fe^{2+}/Mg ratio in the diopsidic pyroxenes and by the Fe^{3+} content in the acmitic members. Paragenesis is discussed briefly.

THIS study of the pyroxenes forms part of an investigation of the alkaline complexes of eastern Uganda. Although considerable variations in optical properties obviously reflect variations in chemical compositions, not only are they difficult to determine accurately owing to the intense colour, but the existing graphs relating optical properties and chemical composition are based on largely inadequate data.

It has been usual to refer to the sodic pyroxenes as aegirine-augite and to regard them as members of the series diopside–aegirine (acmite). In the pyroxenes investigated, however, the third end member, hedenbergite, is of equal importance to the other two.

Mode of occurrence of the pyroxenes. The alkaline complexes of eastern Uganda (fig. 1) consist of two groups: an older group, of presumed Cretaceous age, in which only intrusive rocks are present—these are the complexes of Sukulu, Tororo, Bukusu, Sukululu, and Budeda; and a younger group, of Tertiary age, represented by a series of dissected volcanoes, Kadam, Elgon, Napak, Moroto, and Toror (King and Sutherland, 1960). At Napak, erosion has revealed a central plug of plutonic rocks, while at Toror, the volcanic rocks have been entirely removed, and only the intrusive equivalents are found.

[1] Formerly of Bedford College and of King's College, London.

The chief rock types represented in the complexes are:

Volcanic: melanephelinite–nephelinite (nephelinite series); phonolite–trachyte.

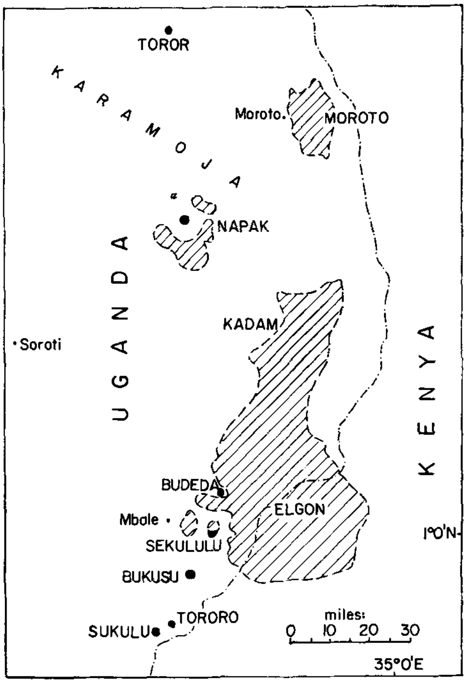

FIG. 1. Sketch map showing the positions of the alkaline complexes in Eastern Uganda. Solid black, intrusive complexes; lined areas, volcanic rocks.

Plutonic: pyroxenite–melteigite–ijolite–urtite (ijolite series)–carbonatite; nepheline-syenite–syenite; and fenite (granite)–syenite–nepheline-syenite.

The principal, and often the only mafic mineral in all of these rocks is a sodic pyroxene, although its abundance varies widely from pyroxenite in which it is almost the sole mineral to the urtites in which it is only sparingly present.

In the volcanic rocks, there is a marked contrast between the diopsidic pyroxenes of the nephelinites and the very aegirine-rich pyroxenes of the phonolites and trachytes. Because of this obvious distinction, and the comparative difficulty of separating the rather small amount of fine-grained pyroxene, a detailed study of the volcanic rocks has been deferred, and in the present account, attention is devoted to the pyroxenes of the plutonic series in which a continuous range of compositions is represented. The pyroxenes of the ijolite series are particularly important, since in these rocks a complicated sequence of events can be recognized (King and Sutherland, 1960; King, 1965). This sequence is: pyroxenite–melteigite–ijolite–ijolite-pegmatite–urtite–wollastonite-urtite.

In addition, the pyroxenes of the nepheline-syenites, carbonatites, and fenites have been studied, but less comprehensively. The majority of the pyroxenes analysed are from the ijolite complex of Lokupoi (Napak), the ijolites and syenites of Budeda, and the carbonatites of Tororo. Four pyroxenes were also analysed from Semarule in Bechuanaland where alkali syenites and fenites occur (King, 1955). It has also been of interest to include reference to two new analyses made of pyroxenes from the Loch Borolan area of northwest Scotland and four from the alkaline rocks of Sørøy, northern Norway. A total of 63 new analyses of pyroxenes from alkali suites have been carried out in the present investigation. Previously published analyses of comparable pyroxenes are few in number, of which a high proportion are aegirine-rich (Sabine, 1950; Pulfrey, 1950; Deer, Howie, and Zussman, 1963).

Chemical composition of the pyroxenes. Zoning is often common in the pyroxenes, and it was necessary therefore to select samples in which zoning was slight or absent. This restricted to some extent the range of samples available. The methods of analysis used were variations of the gravimetric, colorimetric, and flame photometric methods in common use. The results of the analyses, all by R. C. Tyler, are given in table I.

In figs. 2*a* and *b*, plots of $(Mg+Fe^{2+}+Mn)/Ca$ and $(Na+K)/(Fe^{3+}+Ti+Al^{iv})$ are shown from the calculations of the analyses to the formula $X_mY_{2-m}(Si,Al)_2O_6$.

In fig. 3, the pyroxenes have been plotted in terms of the three principal end-members, diopside, hedenbergite, and acmite. The comparatively small amounts of the other constituents justifies the recalculation of the proportions of diopside, hedenbergite, and acmite to 100 %, whereby the compositions of the pyroxenes are shown as points. On this diagram, all the pyroxenes from the African alkaline rocks lie within a curved band extending from near diopside to near acmite. In the most acmitic pyroxenes, the hedenbergite content commonly exceeds that of diopside.

Among minor elements, the content of titanium in the pyroxenes shows

TABLE I. Analyses of pyroxenes from Budeda (B), Bukusu (Bu), Napak (N), Tororo (To) (all in Uganda), Semarule, Bechuanaland (K), Loch Borolan, Scotland (Bo), and Sørøy, Norway (SB).

	B7	B28	B29	B33	B38	B68	B96	B101	B282	Bu414	N23	N30	
SiO_2	50·29	49·30	49·12	49·10	49·59	50·83	50·39	46·08	49·42	51·22	50·30	50·80	SiO_2
TiO_2	1·23	0·78	0·40	1·00	0·51	0·67	1·16	2·51	1·05	0·51	0·39	0·87	TiO_2
Al_2O_3	none	0·27	0·18	0·20	2·43	1·36	2·39	none	none	none	1·28	2·06	Al_2O_3
Fe_2O_3	12·84	9·08	9·48	8·60	7·88	8·86	13·85	13·36	15·33	4·30	9·31	8·80	Fe_2O_3
FeO	10·94	10·45	10·50	10·90	12·05	9·09	10·25	10·96	9·76	7·85	9·54	10·07	FeO
MnO	0·34	0·40	0·42	0·42	0·48	0·48	0·32	0·53	0·64	0·28	0·52	0·32	MnO
MgO	4·68	6·88	6·76	7·37	5·23	5·85	3·16	5·48	3·14	11·21	5·84	4·80	MgO
CaO	15·26	19·12	19·12	20·06	17·61	18·50	12·30	17·27	14·54	23·08	18·49	16·15	CaO
Na_2O	4·36	2·40	2·62	2·60	3·87	3·52	6·25	3·63	6·15	1·54	4·49	3·66	Na_2O
K_2O	0·84	1·04	0·99	0·48	0·45	1·42	0·19	0·21	0·43	0·51	0·27	1·40	K_2O
P_2O_5	trace	0·16	0·14	0·02	0·24	trace	0·06	0·24	trace	none	0·06	0·10	P_2O_5
H_2O+	—	—	—	—	—	—	0·04	—	—	—	—	—	H_2O+
Total	100·78	99·88	99·73	100·75	100·34	100·58	100·36	100·27	100·46	100·50	100·49	99·03	Total
Si	1·955*	1·929†	1·932‡	1·904§	1·934	1·957	1·945	1·836‖	1·954¶	1·943**	1·941††	1·980	Si
Al^{iv}	—	0·014	0·009	0·009	0·066	0·043	0·055	—	—	—	0·058	0·020	Al^{iv}
Al^{vi}	—	—	—	—	0·047	0·017	0·052	—	—	—	—	0·074	Al^{vi}
Ti	—	—	—	—	0·014	0·019	0·035	—	—	—	0·011	0·026	Ti
Fe^{3+}	0·373	0·234	0·232	0·194	0·230	0·254	0·404	0·312	0·340	0·080	0·269	0·258	Fe^{3+}
Fe^{2+}	0·355	0·341	0·345	0·354	0·394	0·293	0·332	0·366	0·316	0·249	0·309	0·328	Fe^{2+}
Mn	0·012	0·014	0·014	0·014	0·016	0·016	0·012	0·017	0·021	0·009	0·016	0·012	Mn
Mg	0·271	0·402	0·397	0·427	0·305	0·336	0·181	0·326	0·181	0·634	0·336	0·279	Mg
Ca	0·635	0·795	0·799	0·834	0·720	0·763	0·508	0·721	0·601	0·939	0·767	0·668	Ca
Na	0·327	0·183	0·199	0·196	0·291	0·263	0·468	0·278	0·460	0·114	0·334	0·277	Na
K	0·042	0·052	0·047	0·023	0·023	0·069	0·009	0·010	0·023	0·023	0·012	0·070	K
X	1·004	1·030	1·045	1·053	1·034	1·095	0·985	1·009	1·084	1·076	1·113	1·015	X
Y	1·012	0·991	0·988	0·989	1·006	0·935	1·016	1·021	0·948	0·972	0·941	0·977	Y
Z	1·990	2·000	2·000	2·000	2·000	2·000	2·000	2·000	2·000	2·000	2·000	2·000	Z
α	1·725	1·711	1·711	1·705	1·719	1·717	1·740	1·720	1·735	1·690	1·719	1·721	α
γ	1·780	1·753	1·753	1·746	1·760	1·773	—	1·758	1·770	1·731	1·759	1·770	γ
A: [001]	22½°	20½°	21½°	20½°	22°	22°	28°	25°	—	—	21°	20°	A: [001]
S.G.	3·45	3·39	3·39	3·40	3·36	3·38	3·48	3·40	3·42	3·40	3·34	3·43	S.G.

B7, Ijolite.
B28, Melteigite.
B29, Melteigite.
B33, Biotite Melteigite.
B38, Ijolite.
B68, Syenitic fenite with nepheline.
B96, Nepheline cancrinite syenite dyke.
B101, Altered ijolite.
B282, Cancrinite syenite.
Bu414, Melteigite.
N23, Medium-coarse grained ijolite with melanite.
N30, Fine-grained ijolite with melanite.

* Also Ti^{iv} 0·035.
† Also Ti^{iv} 0·023, Fe^{3+}(iv) 0·034.
‡ Also Ti^{iv} 0·012, Fe^{3+}(iv) 0·047.
§ Also Ti^{iv} 0·030, Fe^{3+}(iv) 0·057.
‖ Also Ti^{iv} 0·074, Fe^{3+}(iv) 0·090.
¶ Also Ti^{iv} 0·030, Fe^{3+}(iv) 0·016.
** Also Ti^{iv} 0·014, Fe^{3+}(iv) 0·043.
†† Also Ti^{iv} 0·001.

	N32	N35C	N35F	N48	N52	N62	N93	N95	N102	N103C	N103F	N107A	
SiO_2	50·00	51·10	50·73	49·81	50·40	50·29	50·75	50·30	51·36	49·07	49·83	50·10	SiO_2
TiO_2	1·10	1·36	2·35	0·75	0·60	0·86	1·01	1·44	1·08	2·49	1·99	0·59	TiO_2
Al_2O_3	1·46	4·09	3·93	2·21	0·82	4·03	1·09	1·53	4·14	1·51	2·39	none	Al_2O_3
Fe_2O_3	7·70	3·10	4·49	6·57	5·87	2·90	4·37	24·17	21·14	29·69	26·70	15·02	Fe_2O_3
FeO	13·90	3·71	3·97	7·97	9·17	6·07	4·32	5·75	5·00	0·34	1·44	11·35	FeO
MnO	0·71	0·11	0·19	0·22	0·27	0·13	0·18	0·44	0·16	0·29	0·45	0·46	MnO
MgO	2·23	12·24	11·32	8·75	9·47	11·91	12·56	0·78	0·66	1·73	1·06	3·32	MgO
CaO	19·24	21·90	21·40	21·39	20·56	21·67	23·88	5·93	6·75	2·61	2·47	13·12	CaO
Na_2O	3·63	1·10	1·55	2·22	2·34	1·84	1·23	7·59	9·69	11·81	10·62	5·62	Na_2O
K_2O	0·43	0·28	0·18	0·34	0·44	0·35	0·20	1·86	0·49	0·94	1·49	0·85	K_2O
P_2O_5	none	0·01	0·03	0·15	0·32	none	none	0·30	0·03	none	0·13	0·04	P_2O_5
H_2O+	—	—	—	0·02	—	—	—	none	0·02	—	—	—	H_2O+
Total	100·40	99·00	100·14	100·40	100·26	100·05	99·59	100·09	100·52	100·48	98·57	100·47	Total
Si	1·963	1·908	1·879	1·902	1·929*	1·880	1·910†	1·954	1·955	1·886‡	1·944	1·967§	Si
Al^{iv}	0·037	0·098	0·121	0·098	0·037	0·120	0·050	0·046	0·045	0·069	0·056	none	Al^{iv}
Al^{vi}	0·029	0·081	0·053	0·003	—	0·059	—	0·054	0·142	—	0·052	—	Al^{vi}
Ti	0·033	0·038	0·065	0·021	—	0·025	—	0·042	0·030	0·026	0·059	0·016	Ti
Fe^{3+}	0·227	0·085	0·125	0·188	0·154	0·081	0·111	0·704	0·604	0·859	0·783	0·427	Fe^{3+}
Fe^{2+}	0·455	0·116	0·122	0·255	0·294	0·188	0·136	0·187	0·160	0·011	0·047	0·372	Fe^{2+}
Mn	0·024	0·004	0·007	0·007	0·009	0·004	0·007	0·014	0·005	0·009	0·014	0·014	Mn
Mg	0·130	0·680	0·626	0·500	0·540	0·663	0·706	0·047	0·037	0·099	0·061	0·193	Mg
Ca	0·809	0·875	0·850	0·867	0·851	0·867	0·964	0·247	0·277	0·109	0·096	0·552	Ca
Na	0·278	0·081	0·111	0·165	0·175	0·130	0·091	0·569	0·713	0·881	0·802	0·429	Na
K	0·024	0·013	0·009	0·018	0·023	0·017	0·009	0·093	0·023	0·046	0·075	0·042	K
X	1·110	0·969	0·970	1·050	1·049	1·014	1·064	0·909	1·013	1·036	0·973	1·023	X
Y	0·898	1·004	0·998	0·974	0·997	1·020	0·960	1·048	0·978	1·004	1·016	1·006	Y
Z	2·000	2·000	2·000	2·000	2·000	2·000	2·000	2·000	2·000	2·000	2·000	2·000	Z
α	—	1·677	1·684	1·699	1·688	1·696	1·686	1·759	1·763	1·765	1·768	1·736	α
γ	—	1·704	1·720	1·740	1·737	1·731	1·714	—	—	—	—	1·760	γ
A: [001]	—	16½°	16°	20°	19°	14½°	15°	33°	33°	—	—	26°	A: [001]
S.G.	3·46	3·31	3·33	3·35	3·35	3·35	3·37	3·50	3·49	3·50	3·48	3·47	S.G.

N32, Urtite with wollastonite.
N35C, Medium-grained pyroxenite.
N35F, Ijolite.
N48, Medium-grained ijolite.
N52, Medium-grained ijolite.
N62, Melteigite.
N93, Coarse-grained ijolite.
N95, Cancrinite syenite.
N102, Cancrinite syenite.
N103C, Coarse-grained alkali syenite.
N103F, Fine-grained alkali syenite.
N107A, Nepheline syenite.

* Also Ti^{iv} 0·018, Fe^{3+}(iv) 0·016. † Also Ti^{iv} 0·029, Fe^{3+}(iv) 0·011. ‡ Also Ti^{iv} 0·045. § Also Ti^{iv} 0·017.

TABLE I (*cont.*)

	N108	N114	N117	N118	N119	N120R	N120V	N121	N152	N155	N159	N163	N170	
SiO_2	51·40	47·99	50·59	51·70	51·39	51·00	50·50	50·20	49·60	51·00	50·20	50·61	51·80	SiO_2
TiO_2	0·30	1·68	0·63	0·43	0·80	0·85	0·95	0·97	0·91	0·75	0·97	0·68	1·68	TiO_2
Al_2O_3	2·10	none	2·04	2·12	1·86	0·73	2·80	0·89	2·36	2·39	none	2·14	1·91	Al_2O_3
Fe_2O_3	3·63	9·39	8·02	7·05	4·34	4·50	15·48	18·60	2·80	4·95	5·66	4·12	1·92	Fe_2O_3
FeO	8·92	5·37	9·42	9·43	6·98	6·71	7·02	8·58	8·71	6·49	7·66	5·46	4·28	FeO
MnO	0·24	0·19	0·36	0·28	0·18	0·20	0·15	0·42	0·26	0·19	0·26	0·07	0·18	MnO
MgO	9·03	12·00	6·45	5·87	10·95	11·72	4·22	2·88	10·29	9·94	9·85	12·94	13·84	MgO
CaO	20·49	21·18	17·85	18·59	22·45	22·26	12·36	10·42	21·88	21·87	22·09	22·06	23·46	CaO
Na_2O	1·49	1·63	3·40	3·31	1·44	1·66	6·71	6·61	2·11	2·12	1·84	1·58	0·96	Na_2O
K_2O	1·13	0·49	1·22	1·03	0·08	0·20	0·33	0·90	0·49	0·21	1·44	0·28	0·07	K_2O
P_2O_5	—	0·21	none	none	0·03	none	0·05	0·08	none	0·05	0·02	0·01	0·06	P_2O_5
H_2O+	—	none	—	—	—	—	0·03	none	—	—	—	—	none	H_2O+
Total	98·73	100·13	99·98	99·81	100·50	99·83	100·60	100·55	99·35	99·96	99·99	99·95	100·16	Total
Si	1·973	1·842‖	1·949	1·980	1·928	1·931¶	1·928	1·952**	1·901	1·927	1·957*	1·898†	1·916	Si
Al^{iv}	0·027	none	0·051	0·020	0·072	0·032	0·072	0·042	0·099	0·073	none	0·095	0·084	Al^{iv}
Al^{vi}	0·070	—	0·042	0·077	0·009	—	0·052	—	0·007	0·031	—	—	—	Al^{vi}
Ti	0·009	—	0·018	0·012	0·023	—	0·028	0·022	0·025	0·020	—	0·013	0·047	Ti
Fe^{3+}	0·106	0·162	0·231	0·203	0·121	0·115	0·445	0·542	0·083	0·141	0·146	0·117	0·053	Fe^{3+}
Fe^{2+}	0·286	0·173	0·303	0·302	0·219	0·212	0·225	0·278	0·278	0·204	0·246	0·171	0·133	Fe^{2+}
Mn	0·007	0·007	0·012	0·009	0·007	0·006	0·005	0·014	0·007	0·007	0·009	0·002	0·007	Mn
Mg	0·517	0·687	0·370	0·337	0·613	0·662	0·241	0·166	0·587	0·560	0·561	0·724	0·763	Mg
Ca	0·842	0·872	0·736	0·764	0·902	0·903	0·507	0·428	0·899	0·885	0·869	0·886	0·929	Ca
Na	0·111	0·120	0·254	0·245	0·104	0·123	0·495	0·500	0·156	0·154	0·138	0·113	0·067	Na
K	0·055	0·023	0·060	0·051	0·005	0·009	0·018	0·051	0·023	0·009	0·069	0·013	0·004	K
X	1·008	1·015	1·050	1·060	1·001	1·035	1·020	0·979	1·078	1·048	1·076	1·012	1·000	X
Y	0·995	1·029	0·976	0·940	0·992	0·995	0·996	1·022	0·987	0·963	0·962	1·027	1·003	Y
Z	2·000	2·000	2·000	2·000	2·000	2·000	2·000	2·000	2·000	2·000	2·000	2·000	2·000	Z
α	1·696	1·680	1·715	1·713	1·687	1·698	1·733	1·738	1·687	1·693	1·687	1·681	1·660	α
γ	1·734	1·709	1·766	1·760	1·737	1·723	1·780	—	1·730	1·733	1·730	1·720	1·710	γ
A: [001]	17½°	16°	16½°	20°	16°	17½°	—	—	19½°	18½°	16½°	17°	10°	A: [001]
S.G.	3·36	3·35	3·44	3·47	3·33	3·41	—	3·45	3·40	3·38	3·41	3·36	3·32	S.G.

N108, Coarse-grained melanite ijolite.
N114, Ijolite with melanite.
N117, Medium-grained ijolite with melanite.
N118, Fine-grained ijolite.
N119, Variable ijolite.
N120R, Coarse-grained ijolite.
N120V, Vein in coarse-grained ijolite.
N121, Nepheline syenite.
N152, Coarse-grained ijolite.
N155, Medium-grained ijolite.
N159, Medium-grained ijolite.
N163, Schistose ijolite.
N170, Turjaite.

‖ Also Ti^{iv} 0·048, Fe^{3+}(iv) 0·110. ¶ Also Ti^{iv} 0·025, Fe^{3+}(iv) 0·012. ** Also Ti^{iv} 0·006. * Also Ti^{iv} 0·028, Fe^{3+}(iv) 0·015. † Also Ti^{iv} 0·007.

	N178	N511	N514	N516	N517A	N518	N520	N529	N584	To1	To14	To17	To21	
SiO_2	50·56	49·08	50·81	50·49	49·60	50·81	51·03	49·50	50·79	48·18	49·79	50·80	49·61	SiO_2
TiO_2	0·80	1·33	0·58	0·57	0·79	1·23	0·72	1·07	1·29	1·88	1·31	1·13	0·95	TiO_2
Al_2O_3	0·96	2·77	2·37	1·13	0·20	1·16	none	4·94	1·62	1·23	1·46	0·77	none	Al_2O_3
Fe_2O_3	5·52	6·39	4·73	9·06	6·75	4·17	3·75	2·16	8·40	17·03	24·76	24·32	21·20	Fe_2O_3
FeO	11·25	9·60	8·49	11·34	11·84	6·07	5·30	7·35	10·14	6·79	6·04	3·33	6·41	FeO
MnO	0·27	0·36	0·29	0·45	0·39	0·19	0·20	0·19	0·60	0·31	0·22	0·22	0·37	MnO
MgO	6·63	7·93	9·29	5·17	7·72	11·57	13·00	10·90	3·97	3·56	1·62	2·37	2·79	MgO
CaO	19·60	19·48	20·52	19·26	19·24	21·83	23·72	21·74	19·59	13·91	6·11	7·23	10·26	CaO
Na_2O	2·79	2·53	2·25	3·21	2·21	2·04	1·91	1·80	3·50	5·94	8·01	8·89	7·00	Na_2O
K_2O	0·43	0·91	1·02	0·79	1·70	0·69	0·28	1·05	0·25	1·25	0·86	0·40	0·64	K_2O
P_2O_5	0·44	0·17	0·11	0·14	none	0·12	0·04	0·04	none	0·53	trace	0·01	trace	P_2O_5
H_2O+	—	—	—	—	—	—	—	—	—	—	—	—	—	H_2O+
Total	99·25	100·55	100·46	100·61	100·44	99·88	99·95	100·74	100·15	100·61	100·18	99·47	99·23	Total
Si	1·980	1·885	1·927	1·961	1·914‡	1·927§	1·928‖	1·859	1·962	1·894¶	1·934**	1·964*	1·950†	Si
Al^{iv}	0·020	0·115	0·073	0·039	0·009	0·050	—	0·141	0·038	0·056	0·065	0·035	—	Al^{iv}
Al^{vi}	0·022	0·010	0·037	0·012	—	—	—	0·076	0·036	—	—	—	—	Al^{vi}
Ti	0·024	0·038	0·018	0·016	—	0·011	—	0·032	0·037	—	0·036	0·032	—	Ti
Fe^{3+}	0·165	0·184	0·137	0·233	0·140	0·119	0·053	0·063	0·246	0·506	0·723	0·707	0·606	Fe^{3+}
Fe^{2+}	0·370	0·306	0·269	0·369	0·383	0·191	0·168	0·230	0·327	0·224	0·201	0·107	0·210	Fe^{2+}
Mn	0·009	0·011	0·009	0·014	0·012	0·007	0·007	0·007	0·019	0·009	0·007	0·007	0·012	Mn
Mg	0·386	0·454	0·525	0·298	0·442	0·655	0·732	0·609	0·228	0·208	0·093	0·137	0·163	Mg
Ca	0·800	0·793	0·828	0·794	0·773	0·880	0·960	0·875	0·810	0·555	0·282	0·300	0·432	Ca
Na	0·211	0·185	0·164	0·242	0·167	0·150	0·141	0·131	0·260	0·453	0·602	0·665	0·534	Na
K	0·024	0·046	0·050	0·037	0·084	0·031	0·013	0·018	0·014	0·061	0·042	0·019	0·033	K
X	1·035	1·024	1·042	1·073	1·024	1·061	1·114	1·024	1·084	1·069	1·926	0·984	0·999	X
Y	0·976	1·003	0·995	0·942	0·978	0·983	0·960	1·017	0·893	0·954	1·060	0·990	0·991	Y
Z	2·000	2·000	2·000	2·000	2·000	2·000	2·000	2·000	2·000	2·000	2·000	2·000	2·000	Z
α	1·710	1·705	1·699	1·718	1·704	1·689	1·692	1·689	—	1·740	1·756	1·758	1·743	α
γ	1·743	1·760	1·733	1·769	1·763	1·729	1·711	1·729	—	—	—	—	—	γ
A: [001]	19½°	20°	19°	—	20°	16°	13½°	16°	—	26°	29°	31°	25°	A: [001
S.G.	3·45	3·43	3·38	3·42	3·49	3·38	3·32	3·38	3·40	3·47	3·49	3·49	3·40	S.G.

N178, Medium-grained ijolite.
N511, Fine-grained ijolite with melanite and wollastonite.
N514, Coarse-grained ijolite.
N516, Ijolite-pegmatite.

N517A, Ijolite.
N518, Ijolite.
N520, Ijolite.
N529, Pyroxenite.
N584, Urtite.

To1, Syenite.
To14, Carbonate-syenite rock.
To17, Pyroxene-bearing carbonatite.
To21, Pyroxene apatite carbonatite.

‡ Also Ti^{iv} 0·023, Fe^{3+}(iv) 0·054.
** Also Ti^{iv} 0·001.
§ Also Ti^{iv} 0·023.
* Also Ti^{iv} 0·001.
‖ Also Ti^{iv} 0·020, Fe^{3+}(iv) 0·052.
† Also Ti^{iv} 0·028, Fe^{3+}(iv) 0·022.
¶ Also Ti^{iv} 0·059, Fe^{3+}(iv) 0·007.

TABLE I (*cont.*)

	To43	To572	To585	K62	K320	K353	K440	Bo270	Bo330	SB	SB78	SB190	SB245	
SiO_2	51·43	50·86	50·05	49·10	52·15	50·31	48·93	52·00	50·90	51·20	49·20	50·99	50·93	SiO_2
TiO_2	0·37	0·71	0·79	0·37	0·76	0·37	0·57	0·47	0·88	0·27	0·49	0·52	0·45	TiO_2
Al_2O_3	0·21	0·39	2·51	0·20	0·11	none	0·03	1·85	1·00	1·51	2·38	1·97	1·64	Al_2O_3
Fe_2O_3	20·78	16·72	14·32	7·89	28·97	6·73	8·79	9·76	4·66	6·10	8·24	10·69	13·54	Fe_2O_3
FeO	6·55	7·14	9·03	11·91	2·15	6·47	12·96	4·22	8·02	8·01	11·99	6·69	6·49	FeO
MnO	0·94	0·43	0·66	0·51	0·24	0·21	0·61	0·23	0·27	1·03	2·07	0·59	0·94	MnO
MgO	2·63	4·32	2·94	7·12	0·84	11·22	6·71	9·74	10·51	8·66	5·16	6·69	5·65	MgO
CaO	10·43	11·96	13·80	20·25	3·09	22·47	19·71	16·02	21·66	19·54	16·78	15·94	14·37	CaO
Na_2O	6·40	6·32	5·25	2·41	10·75	1·86	2·90	3·82	1·23	2·69	3·36	5·19	6·08	Na_2O
K_2O	0·65	0·98	0·18	0·48	0·22	0·42	0·23	1·37	0·45	0·78	0·87	0·40	0·21	K_2O
P_2O_5	trace	0·17	0·06	0·22	0·27	trace	0·15	0·22	0·14	0·17	0·16	0·08	0·16	P_2O_5
H_2O+	—	—	—	none	—	—	none	—	—	—	—	—	—	H_2O+
Total	100·39	100·50	99·59	100·46	99·55	100·06	101·59	99·70	99·72	99·96	100·70	99·75	100·46	Total
Si	1·988‡	1·962	1·943	1·926§	2·013	1·919‖	1·946¶	1·963	1·938**	1·962	1·921	1·954	1·951	Si
Al^{iv}	0·009	0·038	0·057	0·009	0·005	—	—	0·037	0·046	0·038	0·079	0·046	0·049	Al^{iv}
Al^{vi}	—	0·004	0·060	—	—	—	—	0·045	—	0·031	0·029	0·042	0·025	Al^{vi}
Ti	0·009	0·021	0·023	—	0·023	—	—	0·014	0·009	0·007	0·014	0·016	0·014	Ti
Fe^{3+}	0·604	0·487	0·420	0·178	0·839	0·123	0·221	0·277	0·133	0·175	0·244	0·309	0·392	Fe^{3+}
Fe^{2+}	0·211	0·229	0·294	0·391	0·070	0·206	0·424	0·134	0·256	0·256	0·392	0·214	0·207	Fe^{2+}
Mn	0·030	0·014	0·021	0·016	0·007	0·007	0·021	0·007	0·009	0·035	0·068	0·018	0·030	Mn
Mg	0·150	0·248	0·170	0·417	0·049	0·637	0·351	0·549	0·597	0·495	0·300	0·382	0·322	Mg
Ca	0·432	0·487	0·574	0·834	0·129	0·920	0·773	0·642	0·877	0·794	0·694	0·647	0·583	Ca
Na	0·478	0·473	0·397	0·183	0·803	0·138	0·221	0·281	0·092	0·198	0·253	0·387	0·451	Na
K	0·033	0·046	0·007	0·023	0·009	0·018	0·009	0·068	0·023	0·037	0·042	0·018	0·009	K
X	0·943	1·006	0·980	1·040	0·940	1·075	1·003	0·991	0·992	1·029	0·989	1·052	1·043	*X*
Y	1·004	1·003	0·988	1·002	0·993	0·973	1·017	1·026	1·004	0·999	1·047	0·981	0·976	*Y*
Z	2·000	2·000	2·000	2·000	2·013	2·000	2·000	2·000	2·000	2·000	2·000	2·000	2·000	*Z*
α	1·741	1·736	1·720	1·707	1·765	1·682	1·710	1·711	1·688	1·716	1·728	1·720	1·735	α
γ	—	—	1·770	1·753	—	1·729	1·760	1·741	1·730	1·750	1·770	1·748	1·767	γ
A: [001]	27°	24°	—	18½°	33½°	16°	23°	18°	16½°	—	24½°	22°	24°	A: [001]
S.G.	3·40	3·46	3·48	3·36	3·46	3·33	3·38	3·40	3·37	3·43	3·47	3·45	3·45	S.G.

To43, Syenitic fenite.
To572, Coarse carbonatite.
To585, Pyroxene xenolith in carbonatite.
K62, Syenite pegmatite.
K320, Banded syenite.
K353, Coarse syenite.
K440 Pyroxene schlieren in syenite.
Bo270, Xenolith in borolanite.
Bo330, Cromaltite.
SB, Carbonatite.
SB78, Fenite.
SB190, Nepheline syenite.
SB245, Fenite.

‡ Also Ti^{iv} 0·003. § Also Ti^{iv} 0·012, Fe^{3+}(iv) 0·053. ‖ Also Ti^{iv} 0·011, Fe^{3+}(iv) 0·070. ¶ Also Ti^{iv} 0·016, Fe^{3+}(iv) 0·038. ** Also Ti^{iv} 0·016.

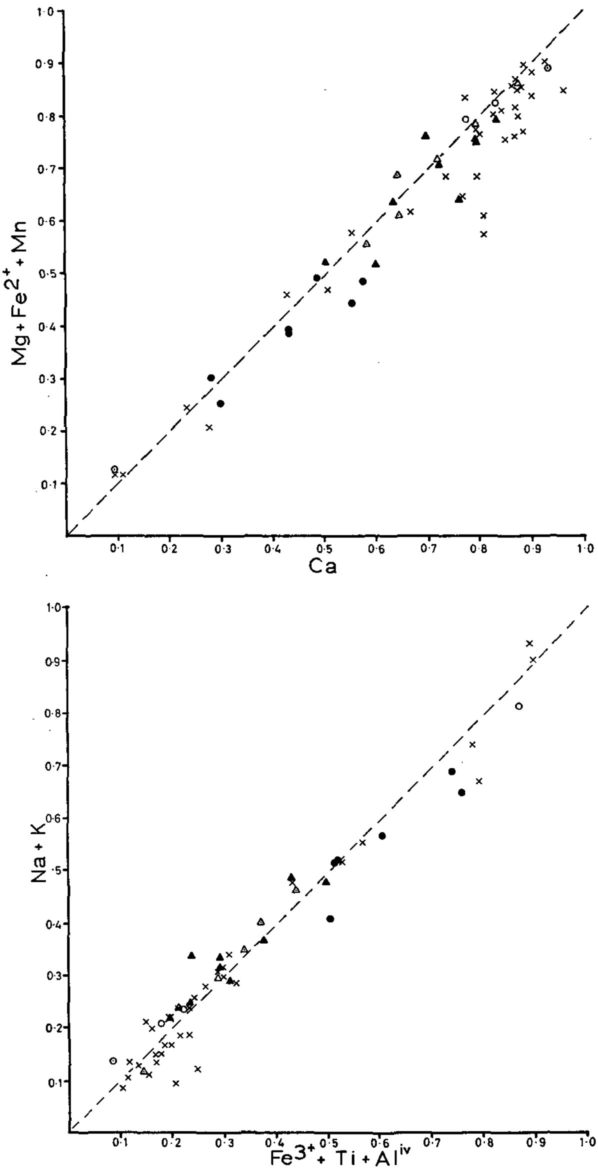

FIG. 2. *a* (top). Plot of $(Mg+Fe^{2+}+Mn)/Ca$ for all the newly analysed pyroxenes. *b* (bottom). Plot of $(Na+K)/(Fe^{3+}+Ti+Al^{iv})$ for all the newly analysed pyroxenes. ▲ Budeda; ⊙ Bukusu; × Napak; ● Tororo; ○ Semarule; △ Sørøy.

dependence on the presence or absence in the rock of other titanium bearing minerals, notably melanite garnet. Titanium is greatest in the pyroxenes from rocks where such minerals are absent (see fig. 4). Manganese increases with increase in the hedenbergite molecule.

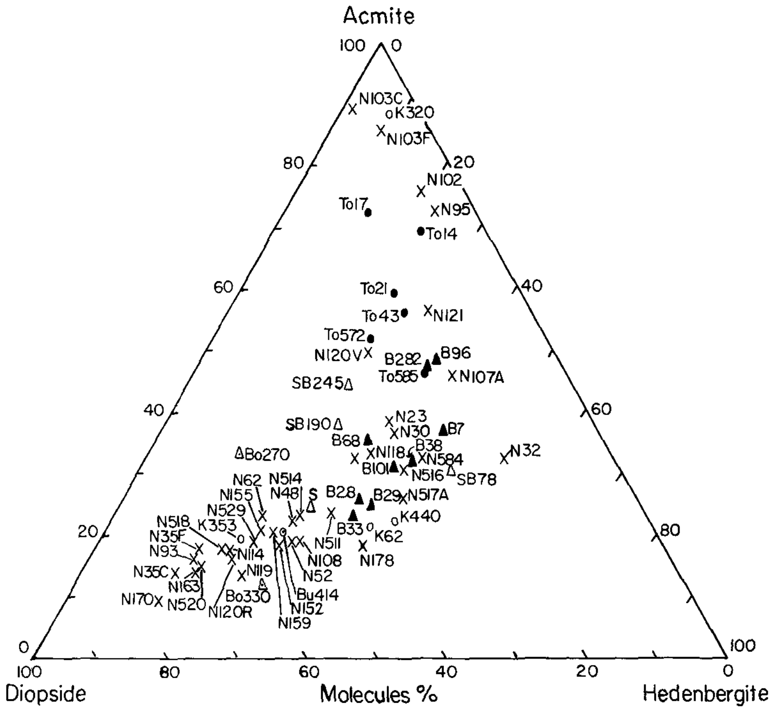

FIG. 3. Pyroxene analyses plotted with diopside + hedenbergite + acmite recalculated to 100 %. Symbols as for fig. 2.

In general, however, titanium, manganese, and also aluminium, vary more in pyroxenes from different regions and localities than among pyroxenes from the same locality; this is shown in table II.

Physical and optical properties of the pyroxenes. The diopsidic pyroxenes are almost colourless; a green colour becomes apparent with an increase in the hedenbergite molecule but becomes particularly noticeable as the content of acmite rises. The variation is readily apparent in zoned crystals. There is some evidence, however, that intensity of colour does not depend solely on the content of the major constituents. It is possible that minor elements have a significant effect not only on the intensity of the colour but also on the shade; for example the pyroxenes from the African complexes are yellowish green in colour, for which the relatively high titanium may be responsible. Other comparable pyroxenes, e.g. Loch Borolan and Sørøy, are a much brighter green.

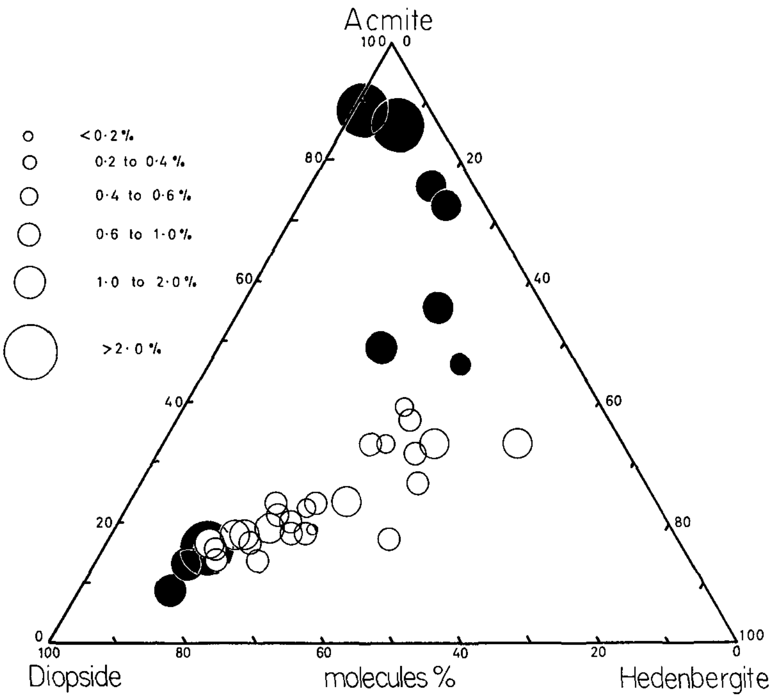

FIG. 4. Content of TiO_2 in the analysed pyroxenes from Napak. Open circles = rocks with melanite, black circles = rocks without melanite.

More difficult to explain is the occurrence of a yellowish-brown variety among the most sodic pyroxenes. Intensity of pleochroism increases with acmite content, but it remains weak in the rather strongly coloured pyroxenes of intermediate composition.

Specific gravities of the pyroxenes increase with the Fe^{2+}/Mg ratio and with the replacement of CaMg by $NaFe^{3+}$. The same chemical factors are responsible for increases in refractive indices and A : [001] angles (see King, 1962).

Physical and optical properties may be used to determine the approximate chemical compositions of pyroxenes in the diopside–hedenbergite–

TABLE II. Analyses recalculated as molecules % of diopside, hedenbergite, acmite, and $CaSiO_3$ or $MgSiO_3$. P_2O_5 calculated out first as apatite taking CaO required from the total. The table also includes actual weights % of MnO, TiO_2, and Al_2O_3 to show variation in these constituents between complexes.

Specimen number	Molecular % Diopside	Hedenbergite	Acmite	$CaSiO_3$	Weight % TiO_2	Al_2O_3	MnO
B.7	26·61	36·32	36·56	0·46	1·23	none	0·34
B.28	38·29	33·63	22·26	5·79	0·78	0·27	0·40
B.29	37·87	36·30	23·30	2·47	0·40	0·18	0·42
B.33	40·23	34·33	20·56	4·81	1·00	0·20	0·42
B.38	28·72	38·14	31·12	1·97	0·51	2·43	0·48
B.68	30·77	28·05	30·35	10·75	0·67	1·36	0·48
B.96	17·04	34·33	47·19	1·40*	1·16	2·39	0·32
B.101	31·11	36·11	29·99	2·70	2·51	none	0·53
B.282	17·28	32·14	42·55	7·98	1·05	none	0·64
Bu.414	59·43	23·98	12·74	3·82	0·51	none	0·28
N.23	25·20	29·17	31·25	14·38	0·39	1·28	0·52
N.30	27·44	32·93	33·85	5·72	0·87	2·06	0·32
N.32	13·82	50·12	15·31	20·74	1·10	1·46	0·71
N.35C	70·64	12·46	9·70	7·16	1·36	4·09	0·11
N.35F	64·91	13·30	12·38	9·40	2·35	3·93	0·19
N.48	47·86	24·66	17·30	10·60	0·75	2·21	0·22
N.52	53·22	28·34	18·18	0·22	0·60	0·82	0·27
N.62	52·20	18·10	18·52	11·15	0·86	4·03	0·13
N.93	65·44	13·13	11·26	10·21	1·01	1·09	0·18
N.95	5·13	22·04	72·00	none	1·44	1·53	0·44
N.102	3·93	16·40	72·06	7·62	1·08	4·14	0·16
N.103C	8·41	1·99	88·49	1·11*	2·49	1·51	0·29
N.103F	5·57	7·97	84·05	2·45*	1·99	2·39	0·45
N.107A	15·96	36·82	44·49	2·69*	0·59	none	0·46
N.108	51·58	28·98	16·43	2·97	0·30	2·10	0·24
N.114	61·70	16·17	13·02	9·03	1·68	none	0·19
N.117	35·36	29·87	29·87	4·83	0·63	2·04	0·36
N.118	31·99	30·69	27·86	9·36	0·43	2·12	0·28
N.119	61·15	22·31	10·70	5·80	0·80	1·86	0·18
N.120R	62·70	20·54	14·98	1·71	0·85	0·73	0·20
N.120V	24·81	23·63	47·75	3·78	0·95	2·80	0·15
N.121	14·08	28·87	54·50	2·54*	0·97	0·89	0·42

Specimen number	Molecular % Diopside	Hedenbergite	Acmite	$CaSiO_3$	Weight % TiO_2	Al_2O_3	MnO
N.152	54·41	26·20	17·36	1·91	0·91	2·36	0·20
N.155	53·65	20·12	15·57	10·60	0·75	2·39	0·19
N.159	52·86	23·85	15·47	7·78	0·97	none	0·26
N.163	67·96	16·21	13·05	2·74	0·68	2·14	0·07
N.170	76·32	13·68	7·51	2·43	1·68	1·91	0·18
N.178	36·86	35·54	22·21	5·33	0·80	0·96	0·27
N.511	44·16	30·79	22·31	2·68	1·33	2·77	0·36
N.514	50·20	26·40	20·76	2·60	0·58	2·37	0·29
N.516	27·66	35·17	26·16	10·94	0·57	1·13	0·45
N.517A	30·68	39·21	21·53	8·53*	0·79	0·20	0·39
N.518	61·99	18·87	16·30	2·78	1·23	1·16	0·19
N.520	67·00	15·88	12·78	4·33	0·72	none	0·20
N.529	57·86	22·56	17·44	2·13	1·07	4·94	0·19
N.584	24·20	35·84	14·42	24·69	1·29	1·62	0·60
To.1	19·08	21·01	46·74	13·08	1·88	1·23	0·31
To.14	8·13	21·90	67·92	1·97*	1·31	1·46	0·22
To.17	13·94	11·58	69·50	4·96	1·13	0·77	0·22
To.21	16·55	22·22	56·75	4·49	0·95	none	0·37
To.43	16·74	25·23	53·37	4·61	0·37	0·21	0·94
To.572	24·65	23·96	51·12	0·23	0·71	0·89	0·43
To.585	17·62	32·15	41·41	8·81	0·79	2·51	0·66
K.62	39·54	38·20	19·54	2·67	0·37	0·20	0·51
K.320	3·72	8·19	86·80	1·24	0·76	0·11	0·24
K.353	57·83	18·99	14·46	8·67	0·37	none	0·21
K.440	35·82	41·53	21·53	1·10*	0·57	0·03	0·61
Bo.270	53·05	13·59	33·32	0·44*	0·47	1·85	0·23
Bo.330	60·43	26·65	11·03	1·83	0·88	1·00	0·27
SB	47·67	27·58	22·96	1·76	0·27	1·51	1·03
SB.78	23·94	45·81	30·21	none	0·49	2·38	2·07
SB.190	36·34	25·32	38·30	none	0·52	1·97	0·59
SB.245	30·69	22·42	43·99	2·83	0·45	1·64	0·94

* $MgSiO_3$, *not* $CaSiO_3$, as in all other instances.

acmite series. Since, however, the pattern of variation in all properties is similar, and depends on the same chemical factors, the composition obtained will be only approximate (see figs. 5 and 6).

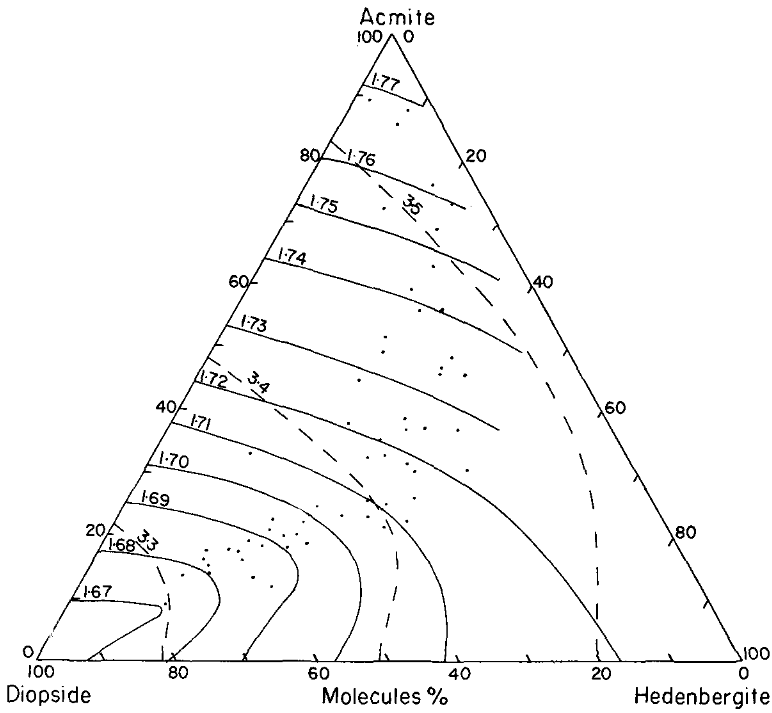

FIG. 5. Diagram showing the variation in specific gravity and the α refractive index of the newly analysed pyroxenes. The positions on diopside–acmite and diopside–hedenbergite are taken from data in Deer, Howie, and Zussman, vol. 2 (1963).

Relation between composition of pyroxene and composition of rock. Petrographic examination shows that the pyroxene of the melanephelinites is a nearly colourless or pale green diopsidic variety. The pyroxene is greener in the more leucocratic rocks, and it is common to find the phenocrysts mantled by narrow zones very rich in acmite. In the phonolites and trachytes, however, a deep green acmitic pyroxene is usual, and the mineral is further characterized by a strongly prismatic or even acicular habit. Occasionally, paler diopsidic cores are present. It is to be inferred that temperature of crystallization (as well as concentration of sodium and iron) is a major factor in determining the composition of the pyroxene, the more acmitic varieties crystallizing at lower temperatures. The sharp compositional difference between diopsidic phenocrysts and their acmitic mantles and ground-mass crystals suggests that these correspond to crystallization under pre-extrusive

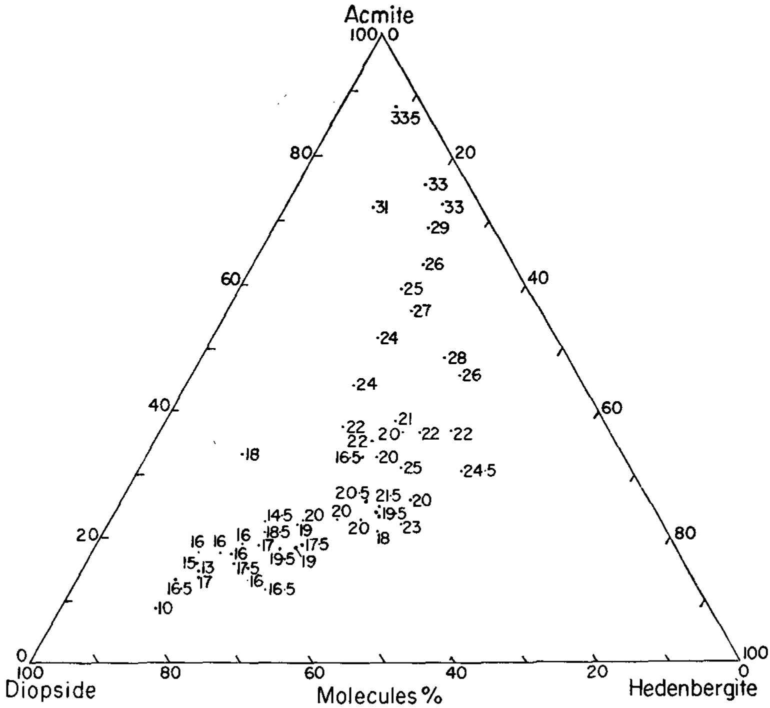

FIG. 6. Diagram showing the variation in the angle A: [001] for the newly analysed pyroxenes. Determinations by B. Collins, B.Sc., Bedford College.

and post-extrusive conditions respectively. Experimental work by Bailey (1963) has shown that the upper temperature-stability limit of acmite increases rapidly as pressures fall to normal. It may be noted that the mineralogy of the nephelinites is very largely represented by the phases in the system acmite–nepheline–diopside investigated by Yagi (1963) and the system albite–nepheline–diopside–acmite–water (Nolan, 1966). The appearance of olivine and melilite as primary crystalline phases over certain compositional ranges at one atmosphere pressure is significant since these are also common minerals in the volcanic rocks.

The pyroxenes of the ijolite series have been studied more fully, and here a continuous range from near diopside to about $Di_{15}He_{55}Ac_{30}$ is shown. Fig. 7 shows that a rather close correlation exists between the composition of the pyroxene and the sequence pyroxenite–melteigite–ijolite–urtite. Field and petrographic studies of the ijolite series shows

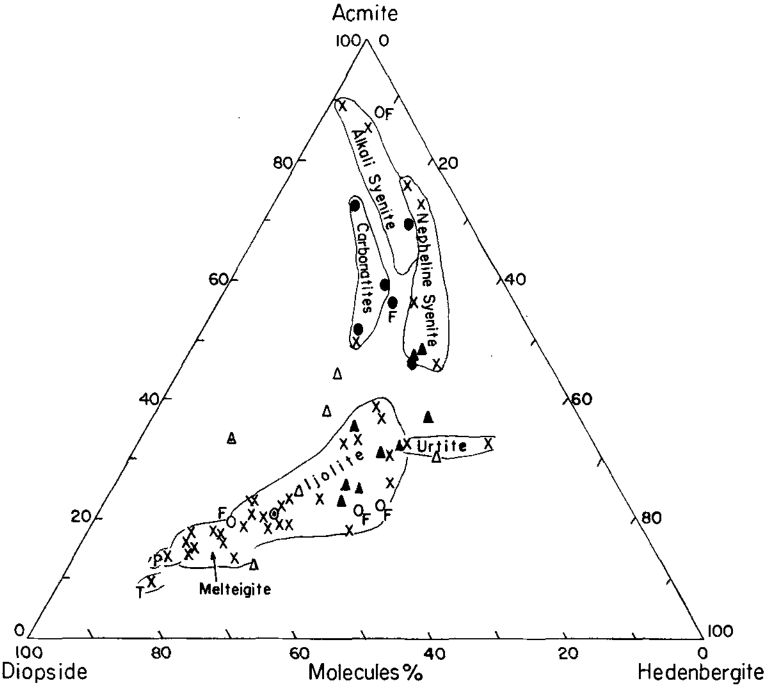

FIG. 7. Diagram showing the variation of the compositions of the newly analysed pyroxenes according to rock type. F = fenite; P = pyroxenite; T = turjaite. Symbols as for fig. 2.

a highly complex sequence of events, which is only very simply represented by the series from pyroxenite to urtite. Critical chemical characteristics of the sequence are expressed by plotting the ratio of total iron oxide to magnesia against that of lime to magnesia as shown in fig. 8 (see also King, 1965). Generally, the hedenbergite–acmite content of the pyroxenes increases in successively later members of the sequence.

Where zoning in the pyroxenes of the ijolite series is shown, it is of two kinds. One is a simple increase in acmite content towards the margins of the crystals corresponding to successive stages of growth.

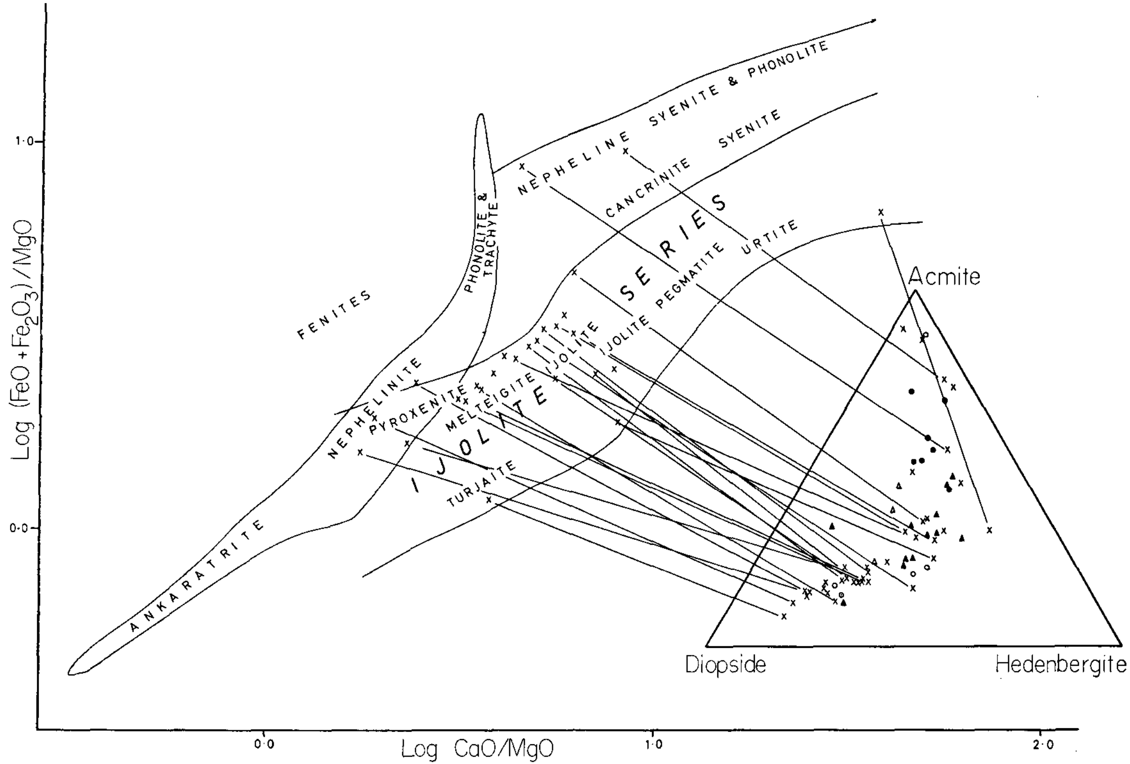

FIG. 8. Plot of log $(FeO+Fe_2O_3)/MgO$ against log CaO/MgO showing that the hedenbergite+acmite content of the pyroxenes increases in successively later members of the Ijolite Series. Symbols in the acmite–diopside–hedenbergite

The second is more patchily developed, and although the acmite content is usually higher towards intergranular boundaries, it is evidently a zoning of metasomatic type, for it is often prominently developed in grains that are adjacent to later veins formed by members of the ijolite sequence (see Napak 120 Rock and Napak 120 Vein).

The compositional range of pyroxenes is extended continuously almost to pure acmite in the nepheline and cancrinite syenites and carbonatites.

The pyroxene series corresponds primarily to a gradient of temperature of formation, the continuity of the series reflecting much greater uniformity of pressure under plutonic conditions than the sudden variations that can be inferred for the volcanic rocks.

The compositions of the pyroxenes in the fenites associated with the alkaline complexes show very wide variations from near diopside to near acmite. Only limited chemical data are yet available, but field and petrographic observations suggest that, although temperature of formation is an important factor, the concentration of sodium and iron may here be of equal importance.

The authors thank Dr. R. A. Howie for his helpful comments.

References

BAILEY (D. K.), 1963. Yearbook Carnegie Inst., vol. 62, p. 131.
DEER (W. A.), HOWIE (R.A.), and ZUSSMAN (J.), 1963. Rock Forming Minerals, vol. 2. London (Longmans).
KING (B. C.), 1955. Syenitisation de granites à Semarule, près de Molepolole, Protectorate de Bechuanaland. C.N.R.S.Coll., Paris, no. 68, p. 1.
—— 1962. Min. Mag., vol. 33, p. 132.
—— 1965. Journ. Petrology, vol. 6, p. 67.
—— and SUTHERLAND (D. S.), 1960. Science Progress, vol. 48, pp. 298 and 503.
NOLAN (J.), 1966. Quart. Journ. Geol. Soc., vol. 122, p. 119.
PULFREY (W.), 1950. Quart. Journ. Geol. Soc., vol. 105, p. 425.
SABINE (P. A.), 1950. Min. Mag., vol. 29, p. 193.
YAGI (K.), 1963. Carnegie Inst. Yearbook, vol. 62, p. 133.

[*Manuscript received 26 April 1966*]